ELSEVIER

International Journal of Refrigeration 22 (1999) 509–520

REVUE INTERNATIONALE DU FROID
INTERNATIONAL JOURNAL OF
refrigeration

www.elsevier.com/locate/ijrefrig

Transport properties of refrigerants R32, R125, R134a, and R125 + R32 mixtures in and beyond the critical region☆

S.B. Kiselev*, R.A. Perkins, M.L. Huber

Physical and Chemical Properties Division, National Institute of Standards and Technology, 325 Broadway, Boulder, CO 80303, USA

Abstract

A practical representation for the transport coefficients of pure refrigerants R32, R125, R134a, and R125 + R32 mixtures is presented which is valid in the vapor–liquid critical region. The crossover expressions for the transport coefficients incorporate scaling laws near the critical point and are transformed to regular background values far away from the critical point. The regular background parts of the transport coefficients of pure refrigerants are obtained from independently fitting pure fluid data. For the calculation of the background contributions of the transport coefficients in binary mixtures, corresponding-states correlations are used. The transport property model is compared with thermal conductivity and thermal diffusivity data for pure refrigerants, and with thermal conductivity data for R125 + R32 mixtures. The average relative deviations between the calculated values of the thermal conductivity and experimental data are less than 4–5% at densities $\rho \geqslant 0.1\rho_c$ and temperatures up to $T = 2T_c$. © 1999 Elsevier Science Ltd and IIR. All rights reserved.

Keywords: Refrigerant; R32; R125; R134a; Thermal conductivity; Thermal diffusivity

Propriétés de transport des frigorigènes R32, R125, R134a et des mélanges de R125 + R32 dans et au-delà la région critique

Résumé

Une représentation pratique des coefficients de transport des frigorigènes purs R32, R125, R134a et des mélanges de R125 et R32 est présentée ; cette représentation s'avère valable dans la région critique vapeur-liquide. Les expressions croisées pour les coefficients de transport comprennent les lois d'étalonnage près du point critique ; loin du point critique, ces valeurs sont transformées en valeurs de fond. Pour les frigorigènes purs, les composants de fond des coefficients de transport sont obtenus à partir de données indépendantes sur les frigorigènes purs. Pour calculer la contribution des valeurs de fond dans les coefficients de transport des mélanges binaires, les corrélations des états correspondants sont utilisées. Le modèle des propriétés de transport est comparé à des données de conductivité et de diffusivité thermiques pour les frigorigènes purs et, dans le cas des mélanges de R125 et R32, à des données de conductivité thermique. Les déviations relatives moyennes entre les valeurs calculées et la conductivité thermique et les données expérimentales sont inférieures à 4 à 5% où les densités se situent à $\rho \geqslant 0.1\rho_c$ et les températures sont inférieures à $T = 2T_c$. © 1999 Elsevier Science Ltd and IIR. All rights reserved.

Mots clés: Frigorigène; R32; R125; R134a; Conductivité thermique; Diffusivité thermique

☆ Contribution of the National Institute of Standards and Technology, not subject to copyright in the United States.

* Corresponding author at present address: Chemical Engineering and Petroleum Refining Department, Colorado School of Mines, Golden, CO 80401-1887, USA. Fax: +1+303-273-370.

E-mail address: skiselev@mines.edu (S.B. Kiselev)

PII: S0140-7007(99)00007-9

1. Introduction

It is important to have accurate values for transport properties such as viscosity and thermal conductivity in order to efficiently design process equipment. There is currently much interest in using mixtures of R125 and R32 to replace R22. R134a has been identified as a possible replacement for R12. Although there are correlations and models available for transport properties of pure fluids as well as mixtures (for example [1–3]), we are unaware of any models for refrigerant mixtures that address the transport properties in the critical region. The present paper provides a practical representation of the transport properties of pure and binary refrigerant mixtures in and beyond the critical region based on the decoupled-mode crossover model for the kinetic coefficients developed by Kiselev et al. [4–8]. This theoretically based model establishes relatively simple yet accurate relationships between the thermodynamic and transport properties of pure fluids and fluid mixtures in the critical region.

Both the viscosity, η, and the thermal conductivity, λ, of fluids are divergent in the vicinity of the gas–liquid critical point [9,10]. The divergence of the thermal conductivity also directly influences the thermal diffusivity, $a - \frac{\lambda}{\rho C_p}$, where ρ is the density and C_p is the isobaric specific heat. The thermal diffusivity of fluids approaches zero at the critical point since C_p diverges more rapidly than λ. The divergence of the viscosity is very localized at the critical point and has little impact on correlations used for refrigeration modeling. However, the critical enhancement of the thermal conductivity is important over the temperature region $0.5T_c \leqslant T \leqslant 1.5T_c$, where T_c, is the critical temperature. Thus, accurate correlations for the thermal conductivity and thermal diffusivity of refrigerants and refrigerant mixtures must address the critical enhancement contribution, both along the saturation boundary and in the supercritical gas. In fact, most of the region of the phase diagram which is relevant to refrigeration processes is close enough to the critical point so that critical enhancement contributes significantly to the thermal conductivity. The situation is further complicated in the case of mixtures of refrigerants since the critical enhancement is not a linear contribution and even the critical point of the specific composition of interest has not been measured and must be calculated based on the properties of the pure fluids in the mixture.

In the vicinity of the critical point, the crossover expression for the critical enhancement of the transport coefficients incorporates the scaling laws and reproduces the asymptotic expressions obtained earlier by Gorodetskii and Gitterman [11] and by Mistura [12,13]. Far from the critical point, the crossover expressions transform into their regular background parts. For the calculation of the regular background transport properties of the pure refrigerants, we use dense-fluid contributions obtained from independently fitting pure fluid data and a dilute-gas contribution from Chapman–Enskog theory. The corresponding scaled equations of state should be used to reproduce the nonanalytic-singular behavior of the kinetic coefficients in the critical region. In the present work, the thermodynamic properties for pure refrigerants R32, R125, R134a, and R125 + R32 mixtures were calculated with a new parametric crossover equation of state developed recently by Kiselev and Huber [14]. This equation of state incorporates the scaling laws asymptotically close to the critical point and transforms into a regular classical expansion far from the critical point.

We proceed as follows. In Section 2, we formulate the crossover equations for the transport coefficients. In Section 3, we propose corresponding states expressions for calculating the regular (background) parts of the kinetic coefficients in binary mixtures. The background transport properties of the pure fluids R32, R125, and R134a are given in Section 4. In Section 5, we compare our crossover model with experimental thermal conductivity and thermal diffusivity data for pure refrigerants R32, R125, R134a, and R125 + R32 mixtures. In Section 6, we discuss our results.

2. Crossover equations for the transport coefficients

To calculate the transport coefficients in pure components and in binary mixtures, we use the crossover expressions obtained by Kiselev et al. [4–8]. In this approach, the Onsager kinetic coefficients of a binary mixture are written in the form

$$\tilde{\alpha} = \frac{k_B T \rho}{6\pi\eta\hat{\xi}} \left(\frac{\partial x}{\partial \mu}\right)_{P,T} \Omega_\alpha(q_D\hat{\xi}) + \tilde{\alpha}_b, \tag{1}$$

$$\tilde{\beta} = \frac{k_B T \rho}{6\pi\eta\hat{\xi}} \left(\frac{\partial x}{\partial T}\right)_{P,\mu} \Omega_\alpha(q_D\hat{\xi}) + \tilde{\beta}_b, \tag{2}$$

$$\tilde{\gamma} = \frac{k_B T^2 \rho}{6\pi\eta\hat{\xi}} \left(\frac{\partial x}{\partial \mu}\right)_{P,T} \left(\frac{\partial \mu}{\partial T}\right)^2_{P,x} \Omega_\alpha(q_D\hat{\xi}) + \frac{k_B T \rho C_{P,x}}{6\pi\eta\hat{\xi}} \Omega(q_D\hat{\xi}) + \tilde{\gamma}_b, \tag{3}$$

where T is the temperature, $\mu = \mu_2 - \mu_1$ is the chemical potential of the mixture, η is the shear viscosity, ρ is the density, $x = N_2/(N_1 + N_2)$ is the mole fraction of the second component, S is the molar entropy of the mixture, ξ is the equilibrium correlation length, and k_B is Boltzmann's constant, and where the subscript b denotes the background part of the kinetic coefficients which are analytic functions of the concentration,

temperature, and density. The crossover functions $\Omega_\alpha(q_D\hat{\xi})$ and $\Omega(q_D\hat{\xi})$ are given by equations

$$\Omega_\alpha(q_D\hat{\xi}) = \frac{2}{\pi}\left[\arctan(q_D\hat{\xi}) - \frac{1}{\sqrt{1+y_D q_D\hat{\xi}}} \times \arctan\frac{q_D\hat{\xi}}{\sqrt{1+y_D q_D\hat{\xi}}}\right], \quad (4)$$

$$\Omega(q_D\hat{\xi}) = \frac{2}{\pi}\left[\arctan(q_D\hat{\xi}) - \frac{1}{\sqrt{1+y_{1d} q_D\hat{\xi}}} \times \arctan\frac{q_D\hat{\xi}}{\sqrt{1+y_{1D} q_D\hat{\xi}}}\right], \quad (5)$$

with

$$y_D = \frac{6\pi\eta^2}{k_B T\rho q_D(\phi_0 + y_0^{-1})}, \quad (6)$$

$$y_{1D} = \frac{6\pi\eta^2}{k_B T\rho q_D(\phi_0 + y_1^{-1})}, \quad (7)$$

where

$$y_0 = \frac{k_B T\rho}{6\pi\eta\hat{\xi}\tilde{\alpha}_b}\left(\frac{\partial x}{\partial\mu}\right)_{P,T}, \quad (8)$$

and

$$y_1 = \frac{k_B T^2\rho}{6\pi\eta\hat{\xi}\tilde{\gamma}_b}\left(\frac{\partial S}{\partial T}\right)_{P,\mu}. \quad (9)$$

In Eqs. (1)–(9) $q_D = |\vec{q}_D|$ is a cutoff wave number and $\phi_0 = \phi(k_D\hat{\xi})$ is the dynamical scaling function [4]

$$\phi(z) = \frac{3[1+z^2+(z^3-z^{-1})\arctan(z)]}{4z^2(1+z^2)} \quad (10)$$

calculated at the constant value of the wave number $k_D = 0.1q_D$ (or $z = 0.lq_D\hat{\xi}$). For the correlation length, we use an expression proposed by Kiselev and Huber [8]

$$\hat{\xi} = \xi_{oz}\exp\left(-\frac{1}{q_D\xi_{oz}}\right), \quad (11)$$

where

$$\xi_{oz} = \xi_0\sqrt{\frac{\tilde{\chi}}{\Gamma_0}} \quad (12)$$

corresponds to the Ornstein–Zernike approximation for the correlation length, and ξ_0 is the amplitude of the asymptotic power law for the correlation length and Γ_0 is the reduced isomorphic compressibility $\tilde{\chi} = \rho(\partial\rho/\partial P)_{T,\mu}P_c\rho_c^{-2}$.

Asymptotically close to the critical point $q_D\hat{\xi} \gg 1$, the singular parts of the kinetic coefficients are much larger than the regular (background) parts ($y_0 \gg 1$, $y_1 \gg 1$, $y_D \approx y_{1D} \approx 1$), all crossover functions approach 1, and Eqs. (1)–(3) in the critical limit reduce to the asymptotic expressions obtained earlier by Gorodetskii and Gitterman [11] and by Mistura [12,13]. Far from the critical point, $q_D\hat{\xi} \ll 1$, the crossover functions approach $0(\Omega_\alpha\xi 0;\ \Omega\xi 0)$, and all kinetic coefficients approach their regular parts.

The thermal conductivity of the mixture λ is defined by [4–7]

$$\lambda = \tilde{\gamma} - T\frac{\tilde{\beta}^2}{\tilde{\alpha}} = \frac{k_B T\rho C_{P,x}}{6\pi\eta\hat{\xi}}\Omega(q_D\hat{\xi}) + \tilde{\alpha}_b\mu_T^2 TQ(y) + \tilde{\gamma}_b, \quad (13)$$

where the crossover function $\Omega_\alpha(q_D\hat{\xi})$ appears only in the argument

$$y = \Delta\tilde{\alpha}/\tilde{\alpha}_b = y_0\Omega_\alpha(q_D\hat{\xi}) = \frac{k_B T\rho}{6\pi\eta\hat{\xi}\tilde{\alpha}_b}\mu_x^{-1}\Omega_\alpha(q_D\hat{\xi}) \quad (14)$$

of the function

$$Q(y) = \frac{y(1+2y^*) - (y^*)^2}{1+y}. \quad (15)$$

Here we have introduced the notation $\mu_x = (\partial\mu/\partial x)_{P,T}$, $\mu_T = (\partial\mu/\partial T)_{P,x}$, and $y^* = \tilde{\beta}_b/(\mu_T\tilde{\alpha}_b)$. In the limit of pure components ($x\vec{\alpha}0$, or $x\vec{\alpha}1$), $\alpha_b \sim x(1-x)\vec{\alpha}0$ [4,7,15], the specific heat capacity $C_{P,x}$ of a binary mixture is transformed to the isobaric specific heat capacity C_P of the pure components, and Eq. (13) for the thermal conductivity of the binary mixtures transforms to the crossover equation for the thermal conductivity of the one-component fluid.

3. Regular parts of the transport coefficients

Eqs. (1)–(9) for the transport coefficients in a binary mixture contain the shear viscosity and the regular (background) parts of the kinetic coefficients, as well as thermodynamic quantities. The viscosity η in these equations represents a shear viscosity which is an analytic function of temperature, density, and concentration. In the present work, we use for the shear viscosity a corresponding-states correlation in the form

$$\eta(T,\rho,x) = \left[\frac{\eta^{(1)}(T,\rho)[T_c^{(1)}]^{1/6}[Z_c^{(1)}]^{2/3}}{\sqrt{M_1}[P_c^{(1)}]^{2/3}}(1-x) + x\frac{\eta^{(2)}(T,\rho)[T_c^{(2)}]^{1/6}[Z_c^{(2)}]^{2/3}}{\sqrt{M_2}[P_c^{(2)}]^{2/3}}\right]\frac{\sqrt{M_{mix}}P_{cx}^{2/3}}{T_{cx}^{1/6}Z_{cx}^{2/3}}, \quad (16)$$

where M_{mix} is the molar mass of the mixture, T_{cx} and P_{cx} are the critical temperature and the critical pressure of the mixture, and the critical compressibility factor $Z_{cx} = P_{cx}/R\rho_{cx}T_{cx}$. The superscripts $i = 1, 2$ denote the components of the mixture and x is the mole fraction of component 2.

The background parts of the kinetic coefficients $\tilde{\alpha}$ and $\tilde{\beta}$ are given by[8]

$$\tilde{\alpha}_b(T, \rho, x) = \tilde{\alpha}_0(T, x) + \tilde{\alpha}_{res}, \tag{17}$$

$$\tilde{\beta}_b(T, \rho, x) = \tilde{\beta}_0(T, x) + \tilde{\beta}_{res}, \tag{18}$$

where $\tilde{\alpha}_0(T, x)$ and $\tilde{\beta}_0(T, x)$ correspond to the dilute-gas parts of the kinetic coefficients, and $\tilde{\alpha}_{res}$ and $\tilde{\beta}_{res}$ are the residual functions. Following Kiselev and Huber [8], the residual functions $\tilde{\alpha}_{res}$ and $\tilde{\beta}_{res}$ (which in general depend on the density, composition and temperature) were treated as functions of the density and composition only:

$$\tilde{\alpha}_{res}(\rho, x) = x(1-x)\frac{R^{-7/6}}{T_{cx}\Gamma_{cx}}\sum_{k=1}^{6}(\alpha_{3k} + \alpha_{3k+1}x) \times \left(\frac{\rho}{\rho_{cx}}\right)^{k+1}, \tag{19}$$

and

$$\tilde{\beta}_{res}(\rho, x) = x(1-x)\frac{R^{-1/6}}{T_{cx}\Gamma_{cx}}\sum_{k=1}^{6}(\beta_{3k} + \beta_{3k+1}x) \times \left(\frac{\rho}{\rho_{cx}}\right)^{k+1}. \tag{20}$$

The background contribution of the kinetic coefficients $\tilde{\gamma}$ is given by [8]

$$\tilde{\gamma}_b = \lambda_0(T, x) + \lambda_{res}^{(1,2)} + T\frac{\tilde{\beta}_b^2(T, \rho, x)}{\tilde{\alpha}_b(T, \rho, x)} + x(1-x)\frac{R^{5/6}}{\Gamma_{cx}}\sum_{k=1}^{6}(\gamma_{2k-1} + \gamma_{2k}x)\left(\frac{\rho}{\rho_{cx}}\right)^{k}, \tag{21}$$

where the composition-dependent coefficient

$$\Gamma_{cx} = \frac{T_{cx}^{1/6}Z_{cx}^{5}\sqrt{M_{mix}}}{P_{cx}^{2/3}}. \tag{22}$$

The residual function $\lambda_{res}^{(1,2)}$ is given by

$$\lambda_{res}^{(1,2)} = \lambda_{res}^{(1)}\frac{[T_c^{(1)}]^{1/6}[Z_c^{(1)}]^5\sqrt{M_1}}{\Gamma_{cx}[P_c^{(1)}]^{2/3}}(1-x) + \lambda_{res}^{(2)}\frac{[T_c^{(2)}]^{1/6}[Z_c^{(2)}]^5\sqrt{M_2}}{\Gamma_{cx}[P_c^{(2)}]^{2/3}}x, \tag{23}$$

where $\lambda_{res}^{(1)}$ and $\lambda_{res}^{(2)}$ define the residual parts of the thermal conductivity λ_b in the limits of the pure components, and the dilute-gas parts of the kinetic coefficients are given by [4–8]

$$\tilde{\alpha}_0 = \frac{\rho D_0 M_{mix}^2}{RT}x(1-x), \tag{24}$$

$$\tilde{\beta}_0 = R\tilde{\alpha}_0\left(\beta_1 + x\beta_2 - \ln\frac{x}{1-x}\right), \tag{25}$$

$$\tilde{\gamma}_0(T, x) = \lambda_0(T, x) + T\frac{\tilde{\beta}_0^2(T, x)}{\tilde{\alpha}_0(T, x)}. \tag{26}$$

In Eqs. (17)–(26), $R = 8314.51$ J kmol^{-1} K^{-1} is the universal gas constant, P_{cx} is in MPa, T_{cx} is in K, $\tilde{\alpha}_b$ is in kg s m^{-3}, $\tilde{\beta}_b$ is in kg m^{-1} s^{-1} K^{-1}, $\tilde{\gamma}_b$ is in W m^{-1} K^{-1}, and α_k, β_k and $\gamma_k (k \geqslant 1)$ are system-dependent coefficients.

For the binary diffusion coefficient in the dilute-gas limit, in Eq. (24), we use an empirical correlation proposed by Fuller et al. [16,17]

$$D_0 = \frac{1.01325 \times 10^{-8}T^{1.75}\left[\frac{M_1 + M_2}{M_1M_2}\right]^{\frac{1}{2}}}{P[(\Sigma v_1)^{\frac{1}{3}} + (\Sigma v_2)^{\frac{1}{3}}]^2}, \tag{27}$$

(where T is in K, P in MPa, and D_0 in m^2 s^{-1}), and for the dilute-gas part of the thermal conductivity $\lambda_0(T, x)$ we use a simple expression proposed by Wassilijeva [18]:

$$\lambda_0(T, x) = \frac{(1-x)\lambda_0^{(1)}(T)}{(1-x) + xA_{12}} + \frac{x\lambda_0^{(2)}(T)}{x + (1-x)A_{21}}, \tag{28}$$

with the Lindsay and Bromley [19] modification for A_{12} and A_{21}:

$$A_{12} = \frac{1}{4}\left\{1 + \left[\frac{\eta^{(1)}(T, 0)}{\eta^{(2)}(T, 0)}\left(\frac{M_2}{M_1}\right)^{\frac{3}{4}}\frac{T + S_1}{T + S_2}\right]^{\frac{1}{2}}\right\}^2\frac{T + S_{12}}{T + S_1},$$

$$A_{21} = \frac{1}{4}\left\{1 - + \left[\frac{\eta^{(2)}(T, 0)}{\eta^{(1)}(T, 0)}\left(\frac{M_1}{M_2}\right)^{\frac{3}{4}}\frac{T + S_2}{T + S_1}\right]^{\frac{1}{2}}\right\}^2\frac{T + S_{12}}{T + S_2}. \tag{29}$$

Here $\lambda_0^{(i)} (i = 1, 2)$ is the thermal conductivity of the pure components in the dilute-gas limit, $S_1 = 1.5T_{nb}^{(1)}$, $S_2 = 1.5T_{nb}^{(2)}$ and $S_{12} = \sqrt{S_1S_2}$ are Sutherland constants, and $T_{nb}^{(1)} (i = 1, 2)$ are the normal boiling temperatures of the pure components.

The correlation length $\hat{\xi}$ is given by Eq. (11), where for the bare correlation length ξ_0 and the cutoff parameter q_D in binary mixtures we use simple linear approximations

$$\xi_0 = \xi_0^{(1)}(1-x) + \xi_0^{(2)}x, \tag{30}$$

$$\frac{1}{q_D} = \frac{1}{q_D^{(1)}}(1-x) + \frac{1}{q_D^{(2)}}x, \tag{31}$$

where superscripts $i = 1, 2$ denote the components of the mixture.

4. Transport coefficients of pure fluids

The background transport properties for R32, R125 and R134a are represented as sums of terms for the temperature-dependent dilute-gas contributions and terms for the temperature- and density-dependent residual contributions. Contributions for the critical enhancement are not included in these background functions. The viscosity is found using

$$\eta(\rho, T) = \eta_0(T) + \eta_{res}(\rho, T), \tag{32}$$

while the thermal conductivity is given by

$$\lambda(\rho, T) = \lambda_0(T) + \lambda_{res}(\rho, T). \tag{33}$$

The dilute-gas viscosity is obtained from kinetic theory [20] assuming that a Lennard–Jones potential applies and using the expression

$$\eta_0(T) = 26.69579 \times 10^{-9} \frac{\sqrt{MT}}{\Omega^{(2,2)}\sigma^2}, \tag{34}$$

where η is in Pa s, M is the molar mass in g mol^{-1}, T is in K, $\Omega^{(2,2)}$ is a collision integral, and σ is the distance, in nm, at which the potential-energy function is 0. The collision integral for a Lennard–Jones potential is evaluated using [21]

$$\Omega^{(2,2)}(t) = \frac{C_1}{t^{C_2}} + C_3 \exp(-C^4 t) + C_5 \exp(-C_6 t), \tag{35}$$

where $C_1 = 1.16145$, $C_2 = 0.14874$, $C_3 = 0.52487$, $C_4 = 0.77320$, $C_5 = 2.16178$, $C_6 = 2.43787$, and $t = k_B T/\epsilon$. The potential energy parameters ϵ and σ for R134a were obtained from [22], while those for R32 and R125 were estimated by a method discussed in [1]. The values are listed in Table 1.

The residual portion of the viscosity is fit to an equation of the form [23]:

$$\eta_{res}(\rho, T) = 10^{-7} \exp\left(a_1 + \frac{a_2}{T}\right) \times \left(\exp\left[\left(a_3 + \frac{a_4}{T^{3/2}}\right)\rho^{0.1} + \left(\frac{\rho}{\rho_c} - 1\right)\rho^{1/2}\left(a_5 + \frac{a_6}{T} + \frac{a_7}{T^2}\right)\right] - 1\right), \tag{36}$$

Table 1
Lennard–Jones potential parameters, ξ_0 and q_D^{-1}, for pure fluids

Tableau 1
Paramètre potentiels de Lennard-Jones ξ_0 et q_D^{-1} pour les frigorigènes purs

Fluid	ϵ/k_B (K)	σ (nm)	ξ_0 (nm)	q_D^{-1} (nm)
R32	262.60	0.4282	0.167	0.8183
R125	250.00	0.5150	0.189	0.8978
R134a	277.74	0.5067	0.194	1.0166

where the residual viscosity is in Pa s, the temperature is in K, and the density is in mol L^{-1}. The coefficients for the residual viscosity for R32 and R125 were found from fitting the experimental data in [24–27] and are listed in Table 2. For R134a we used a viscosity correlation given in [28]. We used the dilute-gas thermal-conductivity correlations from [29,30]:

$$\lambda_0(T) = a_1 + a_2 T + a_3 T^2, \tag{37}$$

where λ_0 is in W m^{-1} K^{-1}, and the coefficients are listed in Table 3. The residual thermal conductivity function is a function of both temperature and density and is given by

$$\lambda_{res}(\rho, T) = [(b_1 + c_1 T)\rho + (b_2 + c_2 T)\rho^2 + (b_3 + c_3 T)\rho^3 + (b_4 + c_4 T)\rho^4], \tag{38}$$

Table 2
Coefficients for the residual viscosity

Tableau 2
Coefficients de viscosité résiduelle

a_i	R32	R125
1	0.3745666×10^{1}	-0.16674402×10^{2}
2	-0.2593564×10^{4}	0.22169228×10^{4}
3	0.3861782×10^{1}	0.17257370×10^{2}
4	0.1807046×10^{5}	-0.25584315×10^{5}
5	0.1478233×10^{1}	0.55675050×10^{-1}
6	-0.5001262×10^{3}	-0.21397030×10^{2}
7	0.5455701×10^{5}	0.24667515×10^{5}

Table 3
Coefficients for the thermal conductivity of the dilute gas

Tableau 3
Coefficients de conductivité thermique du gaz dilué

α_i	R32	R125	R134a
1	0.124363×10^{-1}	-0.200919×10^{-2}	0.579393×10^{-2}
2	-0.628224×10^{-3}	0.330401×10^{-4}	-0.283907×10^{-4}
3	0.199947×10^{-6}	0.669723×10^{-7}	0.176461×10^{-6}

where λ_{res} is in W m^{-1} K^{-1}. The residual thermal conductivity is a weak function of temperature, but a strong function of density. The coefficients for the residual thermal conductivity are given in Table 4.

Table 4
Coefficients for the residual thermal conductivity

Tableau 4
Coefficients de conductivité thermique résiduelle

b_i	R32	R125	R134a
1	0.793100×10^{-2}	0.423907×10^{-3}	0.112233×10^{-1}
2	-0.373196×10^{-3}	0.138085×10^{-2}	-0.449586×10^{-4}
3	0.195280×10^{-4}	-0.171205×10^{-3}	-0.794476×10^{-4}
4	-0.267308×10^{-6}	0.721695×10^{-5}	0.399787×10^{-5}
c_i			
1	-0.129997×10^{-4}	0.282670×10^{-5}	0.362280×10^{-5}
2	0.189222×10^{-5}	-0.187798×10^{-5}	-0.301010×10^{-4}
3	-0.116382×10^{-6}	0.171075×10^{-6}	-0.248613×10^{-6}
4	0.299505×10^{-8}	0.819274×10^{-10}	0.125961×10^{-7}

If the background transport properties of the pure components are known, our crossover model contains two adjustable parameters for each fluid: the bare correlation length $\xi_0^{(i)}$ and the cutoff parameter $q_D^{(i)}$. The parameter $\xi_0^{(i)}$ determines the critical amplitude of the correlation length in the asymptotic critical region and can be independently determined from light-scattering measurements. In the present work, the parameters $\xi_0^{(i)}$ and $q_D^{(i)}$ for pure R32 and R125 have been determined from a fit of our crossover model to experimental thermal-conductivity data only. For pure R134a we adopt the same values for $\xi_0^{(i)}$ as used by Luettmer–Strathmann and Sengers[31,32], while the parameters $q_D^{(i)}$ are determined from a fit of the crossover equation (13) to experimental thermal-conductivity data. The parameters $\xi_0^{(i)}$ and $q_D^{(i)}$ for pure R32, R125, and R134a are presented in Table 1.

The thermal conductivities for pure R32, R125 and R134a along two near-critical isotherms are plotted in Fig. 1. Relative deviations of the calculated thermal conductivities from the experimental values beyond the critical region are shown in Fig. 2. Since the crossover

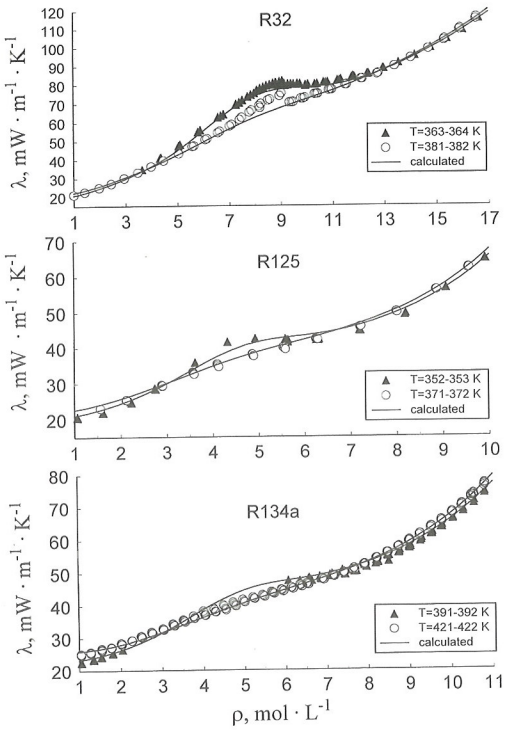

Fig. 1. Thermal conductivities of pure R32, R125 and R134a as a function of the density along isotherms. The symbols indicate experimental data [29] and the curves represent values calculated with the crossover model.

Fig. 1. Conductivités thermiques des frigorigènes purs R32, R125 et R134a en fonction de la densité le long des isothermes. Les symboles indiquent les données expérimentales [29] et les courbes représentent les valeurs calculées à partir du modèle croisé.

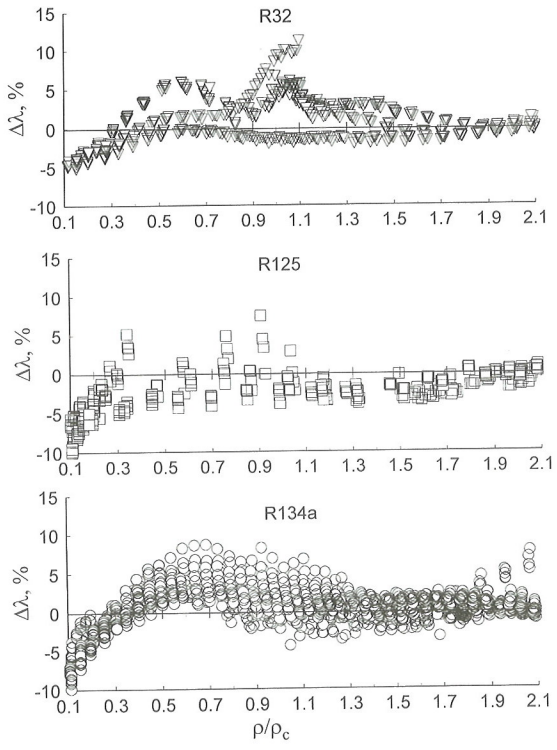

Fig. 2. Relative deviations of experimental thermal conductivity for R32, R125, and R134a [29] from values calculated with the crossover model.

Fig. 2. Déviations relatives de la conductivité thermique expérimentale pour les frigotigènes R32, R125 et R134a [29] à partir de valeurs calculées à partir du modèle croisé.

equations of state used for the calculation of all thermodynamic quantities for pure R32, R125 and R134a [14] do not reproduce the ideal-gas limit at low densities and may even give unphysical behavior as $\rho\vec{\xi}0$, we restrict our calculations to the density region

$$\rho \geqslant 0.1\rho_c. \tag{39}$$

The relative deviations of the thermal conductivity are generally less than 4% over most of the thermodynamic surface, increasing up to 8–10% in the critical region and at the boundary of the region specified by Eq. (39). The experimental values of the thermal diffusivity

$$a = \frac{\lambda}{\rho C_P} \tag{40}$$

for pure R32, R125 and R134a at the coexistence curve [33–35] are compared with calculated values in Figs. 3 and 4. For the calculation of the thermal conductivity we used crossover equation (13), and for the calculation of the density and the specific heat C_P along the coexistence curve we used both the crossover equation of state obtained recently by Kiselev and Huber [14] and the high accuracy analytical equation of state from [36] for R32 and R125, and Ref. [37] for R134a. Far away from the critical point, especially on the vapor side of the coexistence curve, the analytical equations give a better representation of the thermal diffusivity than does the crossover equation [14]. However, the crossover equation must be used in the critical region. The thermal diffusivity for pure R134a in the critical region is shown in Fig. 4 along four supercritical isotherms. Experimental thermal-diffusivity data obtained by Kruppa and Straub [35] agree well with values calculated using the crossover equation.

It is interesting to compare the result of our calculations for pure R134a with the results obtained by Luettmer–Strathmann and Sengers [31,32]. Quantitatively our calculations for the thermal diffusivity in the critical region of R134a, plotted in Figs. 3 and 4, and calculations performed and plotted by Luettmer–Strathmann and Sengers [31,32] reproduce the experimental thermal diffusivity data obtained by Kruppa and Straub [35] with similar accuracy.

5. Thermal conductivities of R125 + R32 mixtures

In order to apply our crossover model to the calculation of the transport properties in binary mixtures, in addition to the equation of state and expressions for the

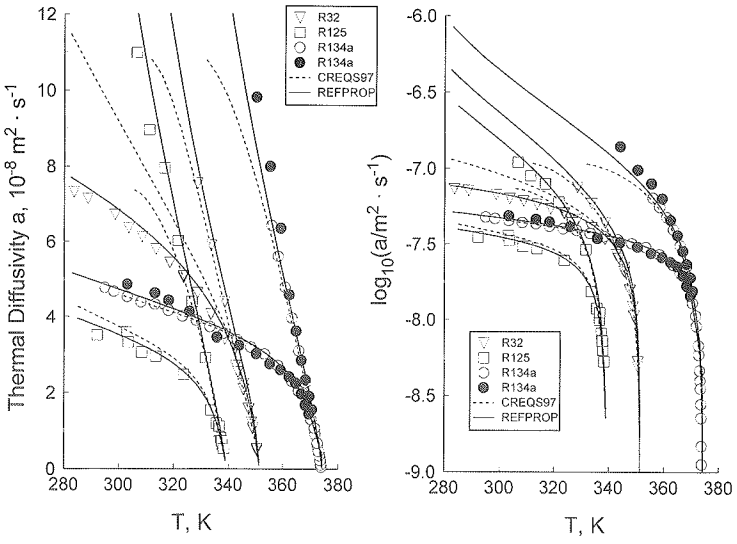

Fig. 3. Thermal diffusivities of pure R32, R125 and R134a along their coexistence curves as a function of the temperature. The open symbols indicate experimental data obtained by Kraft and Leipertz [33,34], and filled symbols correspond to the experimental data obtained by Kruppa and Straub [35] for R134a. The curves represent values of thermal diffusivity calculated with the crossover equation (13) for the thermal conductivity and with the densities and the specific heats calculated with the crossover equation of state [14] (dashed curves), and with analytical equations of state [36,37] (solid curves).

Fig. 3. Diffusivités thermiques des frigorigénes purs R32, R125 et R134a le long de leurs courbes de coexistence en fonction de la température. Les symboles creux indiquent les données expérimentales obtenues par Kraft et Leipertz [33,34] et les symboles remplis correspondent aux données expérimentales obtenues par Kruppa et Straub [35] pour le R134a. Les courbes représentent les valeurs de diffusivité thermique calculées à partir de l'èquation croisée (13) pour la conductivité thermique où les densités et chaleur massique sont calculées à partir de l'équation d'état croisée [14] (courbes hachurées) et à partir des équations d'état analytiques [36,37] (courbes continues).

background transport coefficients for pure components $\lambda_b^{(i)}(T,\rho)$ and $\eta_b^{(i)}(T,p)$, we need also the coefficients a_k, β_k, and γ_k in Eqs. (17)–(21) for the background coefficients $\tilde{\alpha}_b$, $\tilde{\beta}_b$, and $\tilde{\gamma}_b$. The background coefficients $\tilde{\alpha}_b$ and $\tilde{\beta}_b$ determine not only the crossover behavior of the thermal conductivity of a binary mixture in the critical region as given by Eqs. (13)–(15), but also the binary diffusion coefficient

$$D_{12} = \frac{\tilde{\alpha}}{\rho}\mu x, \tag{41}$$

and the thermal diffusion coefficient

$$D_T = \frac{T}{\rho}(\tilde{\alpha}\mu_T + \tilde{\beta}), \tag{42}$$

of binary mixtures far from the critical point. We are not aware of any experimental binary diffusion coefficient data for R125+R32 mixture; therefore, we found the coefficients α_k from fitting the crossover equation (1) together with Eqs. (17) and (41) to binary diffusion coefficient data generated with an empirical correlation for binary fluid mixtures [38]

$$D\eta = \left(D_{12}^0\eta^{(2)}\right)^{x_2}\left(D_{21}^0\eta^{(1)}\right)^{x_1}, \tag{43}$$

where x_1 and x_2 are the mole fractions of the components, and the dilute-solution binary diffusion coefficients D_{12}^0 and D_{21}^0 are calculated with an empirical modification of the Stokes–Einstein equation for the diffusion coefficient [39]

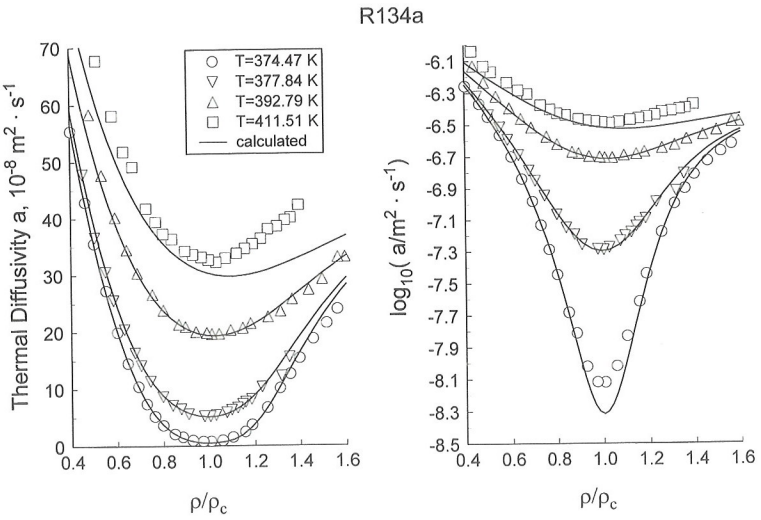

Fig. 4. Thermal diffusivity of pure R134a at supercritical isotherms as a function of the density. The symbols indicate experimental data obtained by Kruppa and Straub [35] and the curves represent values calculated with the crossover model.

Fig. 4. Diffusivité thermique du frigorigène pur R134a à des isothermes supracritiques en fonction de la densité. Les symboles indiquent les données expérimentales obtenues par Kruppa et Straub [35] et les courbes représentent les valeurs calculées à partir du modèle croisé.

Table 5
The background kinetic coefficients α_k, β_k and γ_k used in Eqs. (19)–(21) for R125+R32 mixture

Tableau 5
Coefficient des cinétiques de fond α_k, β_k et γ_k utilisés dans les équations (19) à (21) por le mélange R125+R32

Coefficients for $\tilde{\alpha}_b$		Coefficients for $\tilde{\beta}_b$		Coefficients for $\tilde{\gamma}_b$	
α_6	1.24866×10^{-5}	β_1	2.44626	γ_1	-2.28579×10^{-7}
α_7	-1.02608×10^{-5}	β_3	-7.56262×10^{-6}	γ_2	5.15913×10^{-7}
α_{12}	-1.11600×10^{-5}	β_6	6.51651×10^{-6}	γ_3	1.38394×10^{-6}
α_{13}	1.04080×10^{-5}	β_{12}	-1.18241×10^{-6}	γ_4	-2.67629×10^{-6}
α_{18}	1.39025×10^{-6}	β_{18}	9.64268×10^{-8}	γ_5	-7.35752×10^{-7}
α_{19}	-1.30710×10^{-6}			γ_6	1.35981×10^{-6}
				γ_9	2.14288×10^{-8}
				γ_{10}	-6.56119×10^{-8}

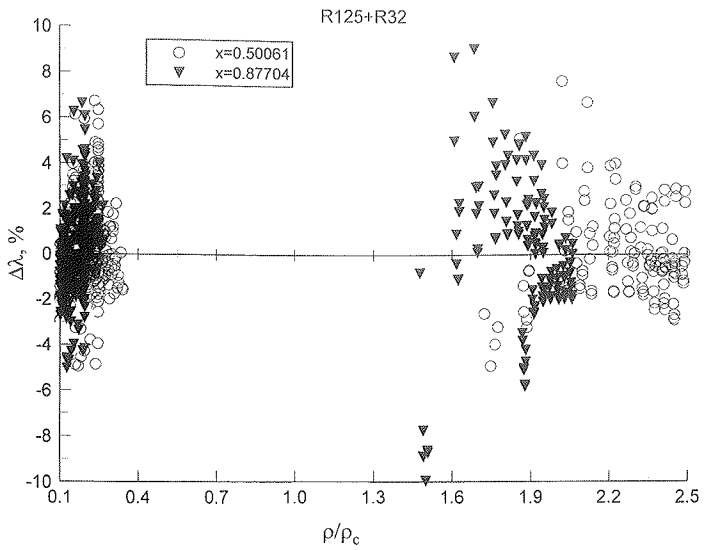

Fig. 5. Relative deviations of experimental thermal conductivity for R125 + R32 mixtures [42] from values calculated with the crossover model at two concentrations of R32.

Fig. 5. Déviations relatives de la conductivité thermique expérimentale pour les mélanges de R125 et R32 [42] à partir de valeurs calculées à partir du modèle croisé, pour deux concentrations de R32.

$$D_{ij}^{0} = \frac{8.5210^{-15} T}{\eta^{(j)} V_j^{\frac{1}{3}}} \left[1.40 + \left(\frac{V_j}{V_i} \right)^{\frac{2}{3}} \right]. \tag{44}$$

Here T is in K, $\eta^{(j)}$ in Pa s, D_{ij}^{0} in $m^2\ s^{-1}$, and V_j and V_i in $cm^3\ mol^{-1}$ are the molar volumes of components at their normal boiling temperatures. These molar volumes are calculated [40] to be

$$V_{R32} = 42.882\,cm^3\,mol^{-1},$$
$$V_{R125} = 79.239\,cm^3\,mol^{-1}. \tag{45}$$

To determine D_0 and λ_0 in Eqs. (24)–(29) for the R125 + R32 mixtures, we use the following values of the atomic diffusion volumes and normal boiling temperatures

$$\Sigma v_{(R32)} = 38.02\,cm^3\,mol^{-1},$$
$$\Sigma v_{(R125)} = 78.88\,cm^3\,mol^{-1}, \tag{46}$$

$$T_{nb}^{(R32)} = 221.49K, \qquad T_{nb}^{(R125)} = 225.01K. \tag{47}$$

The atomic diffusion volumes were calculated using the procedures outlined by Reid et al. [41], while the normal-boiling-point temperatures were obtained from the REFPROP database [40]. Thermodynamic properties for R125 + R32 mixtures were calculated from the new crossover equation of state obtained recently by Kiselev and Huber [14]. The coefficients β_k in the corresponding-states expression (20) for R125 + R32 mixtures were fixed at the same values as in carbon dioxide + ethane mixtures [8]. The coefficients γ_k in Eq. (21) for mixtures R125 + R32 have been found from a fit of the crossover equation (13) (with the values found above for the coefficients α_k), to the experimental thermal-conductivity data. The coefficients α_k, β_k, and γ_k for R125 + R32 mixtures are presented in Table 5. Relative

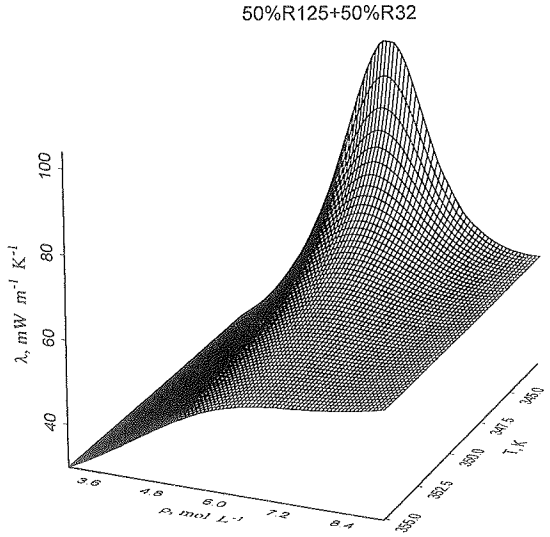

Fig. 6. Thermal conductivity of the 50% R125 + 50% R32 mixture as a function of the temperature and the density in the supercritical region.

Fig. 6. Conductivité thermique du mélange R125 et R32 50%/50% en fonction de la température et la densité dans la région supracritique.

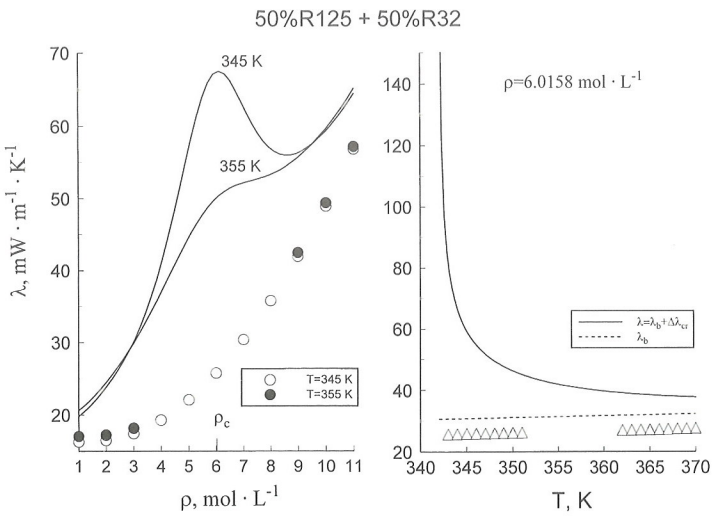

Fig. 7. Thermal conductivity of the 50% R125 + 50% R32 mixture along two isotherms as a function of density (left) and along the critical isochore as a function of the temperature (right). The curves represent values calculated with the crossover model and the symbols indicate values calculated with the program REFPROP V.5 [40]. REFPROP V.5 does not account for the critical enhancement $\Delta\lambda_{cr}$ and shows behavior similar to the background thermal conductivity, λ_b, of the crossover model.

Fig. 7. Conductivité thermique du mélange R125 et R32 50%/50% le long de deux isothermes en fonction de la densité (à gauche) le long de l'isochore critique en fonction de la température (à droite). Les courbes représentent les valeurs calculées à partir du modèle croisé et les symboles indiquent les valeurs calculées à partir du programme REFPROP V.5 [40]. REFPROP V.5 n'explique pas l'augmentation critique $\Delta\lambda_{cr}$ et montre un comportement similaire à celui de la conductivité thermique de fond λ_b du modèle croisé.

deviations of the experimental thermal conductivity from the calculated values for R125 + R32 mixtures are shown in Fig. 5. All experimental thermal conductivity data correspond to temperatures which are near the limits of the range of temperatures, $0.85T_c(x) \leqslant T \leqslant 0.995T_c(x)$, and densities where a good description of the thermodynamic properties of R125 + R32 mixtures was achieved with the crossover equation of state used to calculate the thermodynamic derivatives in Eqs. (13)–(15). However, even in this region the average relative deviations are less than 4–5%. The deviations between the thermal-conductivity data and the crossover model for R125 + R32 mixtures are similar to those found in previous section for pure R32 and R125 (see Fig. 2).

6. Conclusions

We present a model for the transport properties of pure refrigerants R32, R125, R134a, and R125 + R32 mixtures. This model reproduces the scaling-law behavior of the transport coefficients in the critical region and smoothly crosses over to the regular analytical behavior away from the critical region. The regular background transport properties of pure fluids are represented as sums of terms for the temperature-dependent dilute-gas contributions and terms for the temperature and density-dependent residual contributions, which are obtained from independently fitting data for pure fluids. The critical enhancement of the thermal conductivity in pure fluids does not contain any adjustable parameters except for the cutoff wave number $q_D^{(i)}$, and is completely determined by the thermodynamic properties of the system. For the calculation of the thermodynamic quantities of pure refrigerants and R125 + R32 mixtures we use a parametric crossover EOS developed by Kiselev and Huber [14], with parameter $q_D^{(i)}$ determined by fitting our model to experimental thermal conductivity data far from the critical point. Good agreement between experimental and calculated thermal conductivity and thermal diffusivity is observed, both in and beyond the critical region for pure fluids.

In binary mixtures, we calculate the shear viscosity and the background contributions of the kinetic coefficients using corresponding-states correlations. For the density-dependent residual functions of the background parts of the kinetic coefficients $\tilde{\alpha}$, $\tilde{\beta}$ and $\tilde{\gamma}$ we use the same expression as employed earlier by Kiselev and Huber [8]. We are not aware of any experimental data for the binary and thermal diffusion coefficients of the R125 + R32 mixture; therefore, the coefficients α_k were found from a fit of the crossover model to binary diffusion coefficient data generated with an empirical correlation (43). For the coefficients β_k in the corresponding-states expression (20) we adopted the same values as obtained earlier by Kiselev and Huber[8] in carbon dioxide + ethane mixtures. The coefficients γ_k were

found from a fit of the crossover model to the experimental thermal conductivity data of Perkins et al. [42]. The experimental thermal conductivity data [42] for the R125+R32 mixture were obtained in the subcritical region at $T = 331-343$ K, in the density range $\rho \leqslant 0.2\rho_c$ and $\rho \geqslant 1.6\rho_c$, where the critical enhancement of the thermal conductivity $\Delta\lambda_{cr}$ is negligible. Therefore, we cannot compare our model for the R125+R32 mixture with experimental thermal conductivity data in the critical and supercritical region, where a larger critical enhancement of the transport coefficients is expected [4,15]. The thermal conductivity surface for the 50% R125+50% R32 mixture in the critical region calculated with our crossover model is shown in Fig. 6. At the near critical isotherms, $T_c \leqslant T \leqslant 355$ K, the thermal conductivity surface of the 50% R125+50% R32 mixture exhibits singular behavior. A comparison of the thermal conductivity in this region predicted with our model and the values calculated with the computer program NIST REFPROP [41] based on the law of corresponding-states [1,2] is shown in Fig. 7. The computer program NIST REFPROP [40] does not calculate values in the temperature region 353 K $\leqslant T \leqslant$ 363 K at the critical isochore, and in the density range 3 mol L^{-1} $\leqslant \rho \leqslant 9$ mol L^{-1} at $T = 355$ K, since critical enhancement terms were omitted from the model. We found that background contributions for the thermal conductivity predicted with our model are about 8–10 mW m^{-1} K^{-1} larger than the thermal conductivity calculated with the computer program NIST REFPROP [40]. Since there are no experimental data in this region, we do not know which model gives more reliable background values of the thermal conductivity. To resolve this discrepancy, we need more experimental data for the thermal conductivity, as well as binary and thermal diffusion coefficient data for R125+R32 mixtures in the critical and supercritical region.

Acknowledgements

S.B.K. thanks the Physical and Chemical Properties Division, National Institute of Standards and Technology, for the opportunity to work as a Guest Researcher at NIST during the course of this research.

References

[1] Huber ML, Ely JF. Fluid Phase Equilibria 1992;80:239.
[2] Huber ML, Friend DG, Ely JF. Fluid Phase Equilibria 1992;80:249.
[3] Klein SA, McLinden MO, Laesecke A. Int J Refrig 1997;20:208.
[4] Kiselev SB, Kulikov VD. Int J Thermophys 1994;15:283.
[5] Kiselev SB, Povodyrev AA. In: Nagashima A, editor. Proceeding of the 4th Asian Thermophysical Properties Conference, vol. 1. Keio University, Tokyo, 1995. p. 699.
[6] Kiselev SB, Povodyrev AA. High Temp 1996;34:621.
[7] Kiselev SB, Kulikov VD. Int J Thermophys 1997;18:1143.
[8] Kiselev SB, Huber ML. Fluid Phase Equilibria 1998;142:253.
[9] Sengers JV. In: Green MS, editor. Critical phenomena, Varena lectures, course LI. New York, Academic. 1971. p. 445.
[10] Millat J, Dymond JH, Nieto de Castro CA. Transport properties of fluids: their correlation, prediction and estimation. Cambridge: Cambridge University Press, 1996. p. 113–37.
[11] Gorodetskii EE, Gitterman MS. Sov Phys JETP 1970;30:348.
[12] Mistura L. Nuovo Cimento 1972;12B:35.
[13] Mistura L. J Chem Phys 1975;62:4571.
[14] Kiselev SB, Huber ML. Int J Refrig 1998;21:64.
[15] Anisimov MA, Kiselev SB. Int J Thermophys 1992;13:873.
[16] Fuller EN, Giddings JC. J Gas Chromatogr 1965;3:222–7.
[17] Fuller EN, Schettler PD, Giddings JC. Ind Eng Chem 1966;58(5):18.
[18] Wassilijeva A. Physik Z 1894;5:737.
[19] Lindsay AL, Bromley LA. Ind Eng Chem 1950;42:1508.
[20] Hirschfelder JO, Curtiss CF, Bird RB. Molecular theory of gases and liquids. New York: Wiley & Sons, 1953.
[21] Neufeld PD, Janzen AR, Aziz RA. J Chem Phys 1972;57:1100.
[22] Nabizadeh H, Mayinger F. Proc 12th European Conference on Thermophysical Properties, Vienna (Austria), 1990.
[23] Holland PM, Hanley HJM. J Phys Chem Ref Data 1979;8:559.
[24] Diller DE, Peterson SM. Int J Thermophys 1993;14:55.
[25] Oliveira CMP, Wakeham WA. Int J Thermophys 1993;14:1131.
[26] Takahashi M, Shibasaki-Kitakawa N, Yokoyama C, Takahashi S. J Chem Eng Data 1995;40:900–2.
[27] Ripple D, Matar O. J Chem Eng Data 1993;38:560.
[28] Laesecke A. J Physical and Chemical Ref Data, submitted for publication.
[29] Perkins RA, Laesecke A, Howley J, Nieto de Castro CA. Experimental thermal conductivity and thermal diffusivity values for R32, R125, and R134a. NIST IR, submitted for publication.
[30] Perkins RA, Howley J, Ramires MLV, Gurova AN, Cusco L. Experimental thermal conductivity and thermal diffusivity values for the IUPAC round-robin sample of 1,1,1,2-tetrafluoroethane (R134a). NIST IR, submitted for publication.
[31] Krauss R, Luettmer-Strathmann J, Sengers JV, Stephan K. Int J Thermophys 1993;14:951.
[32] Luettmer-Strathmann J, Sengers JV. High Temp–High Press 1994;26:673.
[33] Kraft K, Leipertz A. Proc Int Conf CFCs, The Day After, Padova (Italy), 21–23 September 1989. p. 435.

[34] Kraft K, Leipertz A. Int J Thermophys 1994;15:387.
[35] Kruppa B, Straub J. Fluid Phase Equilibria 1992;80:305.
[36] Outcalt SL, McLinden MO. Int J Thermophys 1995;16:79.
[37] Huber ML, Ely JF. Int J Refrigeration 1994;17:18.
[38] Leffler J, Gullinan HT. Ind Eng Chem Fundam 1970;9:84.
[39] Lusis MA, Ratcliff GA. Can J Chem Eng 1968;46:385.
[40] NIST thermodynamic properties of refrigerants and refrigerant mixtures database, V5.0. NIST SRD no. 23, 1996.
[41] Reid RC, Prausnitz JM, Sherwood TK. The properties of gases and liquids. New York: McGraw–Hill, 1977.
[42] Perkins RA, Laesecke A, Howley J. Experimental thermal conductivity and thermal diffusivity values for mixtures of R32 and R134a. NIST IR, submitted for publication.